RESEARCH ARTICLE OPEN ACCESS

Closed Loop Speed Control of a BLDC Motor Drive Using Adaptive Fuzzy Tuned PI Controller

Sri Latha Eti[1] , Dr. N. Prema Kumar[2]
[1]PG Scholar, Dept. of Electrical Engineering, A.U College of Engineering (A), Andhra University, Visakhapatnam, A.P, India
[2] Associate Professor, Dept. of Electrical Engineering, A.U College of Engineering (A), Andhra University, Visakhapatnam, A.P, India

ABSTRACT
Brushless DC Motors are widely used for many industrial applications because of their high efficiency, high torque and low volume. This paper proposed an improved Adaptive Fuzzy PI controller to control the speed of BLDC motor. This paper provides an overview of different tuning methods of PID Controller applied to control the speed of the transfer function model of the BLDC motor drive and then to the mathematical model of the BLDC motor drive. It is difficult to tune the parameters and get satisfied control characteristics by using normal conventional PI controller. The experimental results verify that Adaptive Fuzzy PI controller has better control performance than the conventional PI controller. The modeling, control and simulation of the BLDC motor have been done using the MATLAB/SIMULINK software. Also, the dynamic characteristics of the BLDC motor (i.e. speed and torque) as well as currents and voltages of the inverter components are observed by using the developed model.

Keywords - BLDC motor, Motor drive, Conventional P, PI, PID Controllers, Different PID Tuning methods, Adaptive fuzzy PI Controller

I. INTRODUCTION

Permanent magnet brushless DC motors (PMBLDC) find wide applications in industries due to their high power density and ease of control. These motors are generally controlled using a three phase power semiconductor bridge. For starting and the providing proper commutation sequence to turn on the power devices in the inverter bridge the rotor position sensors are required. Based on the rotor position, the power devices are commutated sequentially every 60 degrees. To achieve desired level of performance the motor requires suitable speed controllers. In case of permanent magnet motors, usually speed control is achieved by using proportional-integral (PI) controller. Although conventional PI controllers are widely used in the industry due to their simple control structure and ease of implementation, these controllers pose difficulties where there are some control complexity such as nonlinearity, load disturbances and parametric variations. Moreover PI controllers require precise linear mathematical models. Fuzzy Logic Controller (FLC) for speed control of a BLDC leads to an improved dynamic behavior of the motor drive system and immune to load perturbations and parameter variations.

II. BLDC MOTOR MODELLING

2.1Simulation of BLDC motor

Brushless Direct Current (BLDC) motors are one of the motor types rapidly gaining popularity. BLDC motors are used in industries such as Appliances, Automotive, Aerospace, Consumer, Medical, Industrial Automation Equipment and Instrumentation. As the name implies, BLDC motors do not use brushes for commutation; instead, they are electronically commutated. BLDC motors have many advantages over brushed DC motors and induction motors as in [1]. A few of these are better speed vs torque characteristics, high dynamic response, high efficiency, long operating life and noiseless operation.

In addition, the ratio of torque delivered to the size of the motor is higher, making it useful in applications where space and weight are critical factors. The BLDC motor is supplied from battery through the inverter. The dynamic model of this system is shown in Fig.1. It is derived under the following assumptions[2]:

- All the elements of the motor are linear and core losses are neglected.
- Induced currents in the rotor due to stator harmonic fields are neglected.
- The electromotive force e_a varies sinusoidal with the rotational electric angle θ_e.
- The cogging torque of the motor is negligible.

- Due to the surface mounted permanent magnets, winding inductance is constant (doesn't change with the rotor angle).
- Voltage drop across the diodes, thyristors and the connecting wires are ignored.

All above mentioned assumptions are practically satisfied. The magnetic and electric circuit is linear within the range of operation. Power losses in the inverter are practically negligible since the switching frequency of this low speed motor is low. Also the cogging torque doesn't exist since there is coreless winding.

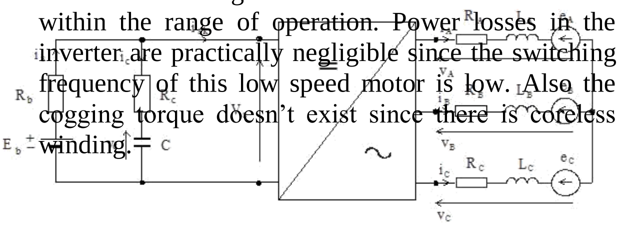

Fig.1. Circuit diagram of supply-inverter-motor system

The equations that describe the model are as follows:

$$V_s = E_b - i_s.R_b - i_c.R_c \quad (1)$$

$$V_s = V_c + i_c.R_c \quad (2)$$

$$i_s = i_{sk} + i_c \quad (3)$$

where:

E_b and R_b – voltage and resistance of the source (battery)

R_c – resistance in the capacitor circuit

i_s – source circuit current

i_{sk} – converter input current

V_c – voltage across capacitor

$$V_c = \frac{Q_c}{C} \quad (4)$$

Q_c– Charge in the capacitor

C – Capacitance

i_c - Current flowing through the capacitor

$$i_c = \frac{dQ_c}{dt} \quad (5)$$

The equation across the motor winding

$$\begin{bmatrix} V_a \\ V_b \\ V_c \end{bmatrix} = \begin{bmatrix} R_a & 0 & 0 \\ 0 & R_b & 0 \\ 0 & 0 & R_c \end{bmatrix} \begin{bmatrix} i_a \\ i_b \\ i_c \end{bmatrix} + \frac{d}{dt} \begin{bmatrix} L_a & L_{ab} & L_{ac} \\ L_{ba} & L_b & L_{bc} \\ L_{ca} & L_{cb} & L_c \end{bmatrix} \begin{bmatrix} i_a \\ i_b \\ i_c \end{bmatrix} + \begin{bmatrix} e_a \\ e_b \\ e_c \end{bmatrix} \quad (6)$$

Or in shorter version

$$V_a = R_a.I_a + L_a\frac{dI_a}{dt} + e_a \quad (7)$$

Since the resistances of all the phases are equal

$$R_a = R_b = R_c \quad (8)$$

Here

L_a, L_b and L_c are the self inductances of phases a, b, c;

L_{ab}, L_{bc} and L_{ca} are the self inductances of phases a, b, c;

e_a, e_b and e_c are the phase back electromotive forces;

Since the self- and mutual inductances are constant for surface mounted permanent magnets and the winding is symmetrical:

$$L_a = L_b = L_c = L \quad (9)$$

$$L_{ab} = L_{ba} = L_{ca} = L_{ac} = L_{bc} = L_{cb} = M$$

Substituting equations (8), and (9) equation (6) gives the BLDCM model as

$$\begin{bmatrix} V_a \\ V_b \\ V_c \end{bmatrix} = \begin{bmatrix} R_a & 0 & 0 \\ 0 & R_a & 0 \\ 0 & 0 & R_a \end{bmatrix} \begin{bmatrix} i_a \\ i_b \\ i_c \end{bmatrix} + \frac{d}{dt} \begin{bmatrix} L & M & M \\ M & L & M \\ M & M & L \end{bmatrix} \begin{bmatrix} i_a \\ i_b \\ i_c \end{bmatrix} + \begin{bmatrix} e_a \\ e_b \\ e_c \end{bmatrix} \quad (10)$$

The stator phase currents are constrained to be balanced i.e.

$$i_a + i_b + i_c = 0 \quad (11)$$

This leads to the simplifications of the inductances matrix in the models as the

$$Mi_b + Mi_c = -Mi_a \quad (12)$$

Therefore in the state space form

$$\begin{bmatrix} V_a \\ V_b \\ V_c \end{bmatrix} = \begin{bmatrix} R_a & 0 & 0 \\ 0 & R_a & 0 \\ 0 & 0 & R_a \end{bmatrix} \begin{bmatrix} i_a \\ i_b \\ i_c \end{bmatrix} + \frac{d}{dt} \begin{bmatrix} L-M & 0 & 0 \\ 0 & L-M & 0 \\ 0 & 0 & L-M \end{bmatrix} \begin{bmatrix} i_a \\ i_b \\ i_c \end{bmatrix} + \begin{bmatrix} e_a \\ e_b \\ e_c \end{bmatrix} \quad (13)$$

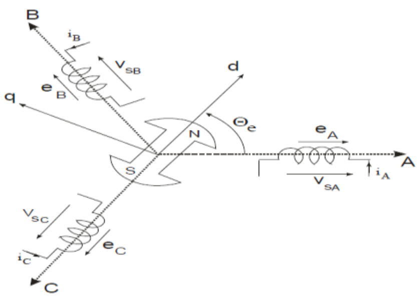

Fig.2 Position of the rotor with respect to the phase A

The electromotive force induced in the phase *A* winding is

$$e_a = K_e \omega_m f_a(\theta_e) \quad (14)$$

where:

K_e – Constant, ω_m – rotor angular speed

$$\omega_m = \frac{2}{P}\frac{d\theta_e}{dt} \quad (15)$$

θ_e – Electrical angle (from fig.2)

P – Number of pole pairs

For three-phase winding the electromotive forces written in the form of a matrix

$$\begin{bmatrix} e_a \\ e_b \\ e_c \end{bmatrix} = E \begin{bmatrix} f_a(\theta_e) \\ f_b(\theta_e) \\ f_c(\theta_e) \end{bmatrix} \quad (16)$$

where, ($E=K_e.\omega_m$)

Motion equation:

$$T_J + T_D + T_S + T_L = T_e \quad (17)$$

where,

Torque due to Inertia, $T_J = J\frac{d\omega_r}{dt}$ where, *J* – Moment of inertia,

Torque due to viscous friction, $T_D = B.\omega_r$, where, *B* – Friction coefficient,

Torque due to Coulomb friction, $T_s = \sin(\omega_r)T_d$ and, laod torque T_L

Electromagnetic torque for 3-phase motor

$$T_e = \frac{e_a i_a}{\omega_m} + \frac{e_b i_b}{\omega_m} + \frac{e_c i_c}{\omega_m} \quad (18)$$

$$T_e = K_e\left(f_a(\theta_e).\,i_a + f_b(\theta_e).\,i_b + f_c(\theta_e).\,i_c\right) \quad (19)$$

2.2 Modelling of Trapezoidal Back emf equations

The trapezoidal back emf waveforms are modeled as a function of rotor position so that the rotor position can be actively calculated according to the operation speed[3]. The back emfs are expressed as a function of rotor position (θ_e), which can be written as:

$$\begin{bmatrix} e_a \\ e_b \\ e_c \end{bmatrix} = E \begin{bmatrix} f_a(\theta_e) \\ f_b(\theta_e) \\ f_c(\theta_e) \end{bmatrix} \quad (20)$$

where,

$$f_a(\theta_e) = \begin{cases} \frac{6}{\pi}\theta & 0 \le \theta \le \pi/6 \\ 1 & \pi/6 \le \theta \le 5\pi/6 \\ \frac{-6}{\pi}\theta + 6 & 5\pi/6 \le \theta \le 7\pi/6 \\ -1 & 7\pi/6 \le \theta \le 11\pi/6 \\ \frac{6}{\pi}\theta - 12 & 11\pi/6 \le \theta \le 2\pi \end{cases}$$

$$f_b(\theta_e) = \begin{cases} -1 & 0 \le \theta \le \pi/2 \\ \frac{6}{\pi}\theta - 4 & \pi/2 \le \theta \le 5\pi/6 \\ 1 & 5\pi/6 \le \theta \le 9\pi/6 \\ \frac{-6}{\pi}\theta + 10 & 9\pi/6 \le \theta \le 11\pi/6 \\ -1 & 11\pi/6 \le \theta \le 2\pi \end{cases} \quad (21)$$

$$f_c(\theta_e) = \begin{cases} 1 & 0 \le \theta \le \pi/6 \\ \frac{-6}{\pi}\theta + 2 & \pi/6 \le \theta \le \pi/2 \\ -1 & \pi/2 \le \theta \le 7\pi/6 \\ \frac{6}{\pi}\theta - 8 & 7\pi/6 \le \theta \le 9\pi/6 \\ 1 & 9\pi/6 \le \theta \le 2\pi \end{cases}$$

The trapezoidal back emf waveforms of a BLDC motor are realized using trapezoidal shape function of rotor position with limit values between +1 and -1 using Embedded matlab function.

2.3 Three phase Voltage source Inverter

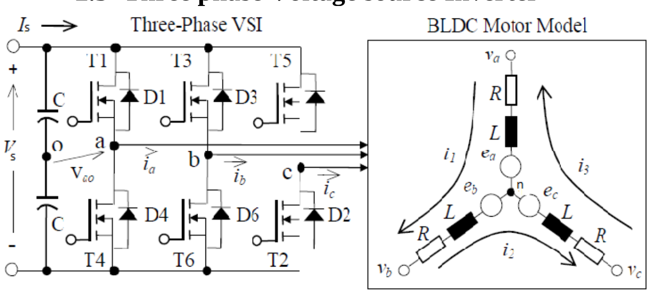

Fig.3 Configuration of BLDC motor and Three Phase VSI system

Three phase bridge inverters are widely used for ac motor drives and general purpose ac supplies. The input dc supply is usually obtained from a battery or from a single phase or three phase utility power supply through diode bridge rectifier and LC or C filter as shown in Fig.3. The capacitor tends to make the input dc voltage constant. This also suppresses the harmonics fed back to the dc source.

These output voltages are plotted as shown in Fig. 4 below. The output voltages obtained of the three phase VSI can be expressed in terms of switching functions S_a, S_b and S_c obtained from the hysteresis current controller as below:

When the IGBTs in the upper half of the Inverter conduct, i.e., when T_1, T_3 and T_5 conduct, the switching functions output will be 1 and when T_2, T_4 and T_6 conduct, the switching functions return 0 as output.

The inverter output voltages are thus obtained as

$$\begin{aligned} v_{an} &= \frac{1}{3}(2S_a - S_b - S_c) \times V_s \\ v_{bn} &= \frac{1}{3}(2S_b - S_a - S_c) \times V_s \\ v_{cn} &= \frac{1}{3}(2S_c - S_a - S_b) \times V_s \end{aligned} \quad (22)$$

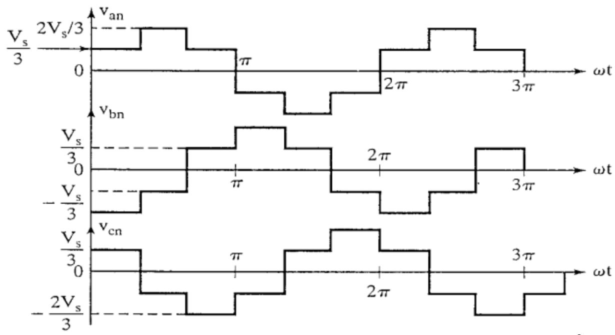

Fig.4 Three phase output voltages on a three-phase VSI in 180^0 mode

2.4 Current Controller

The commanded value of current is compared to the actual phase currents of the motor and the errors are processed through a current controller as in [4].

The current controller can be of two types:

1) PWM Current controller
2) Hysteresis current controller

Due to variable switching frequency, adjustable ripple currents and fastest response, Hysteresis current controller is chosen instead of a PWM current controller.

The magnitude of the commanded value of current i_{ref} is determined by using the reference torque T_{ref} as

$$i_{ref} = \frac{T_{ref}}{K_t} \quad (23)$$

where, K_t is the torque constant.

Depending on the rotor position, the three phase reference currents are obtained by taking the value of reference current magnitude as i_{ref}. The table 1 below gives the dependency of the three phase reference currents on the rotor position.

The Hysteresis current controller contributes to the generation of the switching signals for the three phase Voltage Source Inverter. The controller continuously compares the actual three phase currents with the reference currents generated within the hysteresis band.

TABLE I. ROTOR POSITION AND THREE PHASE REFERENCE CURRENTS

Rotor position ( )	Reference Currents		
	i_{aref}	i_{bref}	i_{cref}
$0-30$	0	$-i_{ref}$	i_{ref}
$30-90$	i_{ref}	$-i_{ref}$	0
$90-150$	i_{ref}	0	$-i_{ref}$
$150-210$	0	i_{ref}	$-i_{ref}$
$210-270$	$-i_{ref}$	i_{ref}	0
$270-330$	$-i_{ref}$	0	i_{ref}
$330-360$	0	$-i_{ref}$	i_{ref}

If $i_a \le i_{aref} - hb;\quad set\ S_a = 1$
$i_a \ge i_{aref} + hb;\quad set\ S_a = 0$

Similarly,
If $i_b \le i_{bref} - hb;\quad set\ S_b = 1$
$i_b \ge i_{bref} + hb;\quad set\ S_b = 0$ (24)

and,
If $i_c \le i_{cref} - hb;\quad set\ S_c = 1$
$i_c \ge i_{cref} + hb;\quad set\ S_c = 0$

These switching functions serve as the input to the three phase VSI.

2.5 Speed Controller

The closed loop speed regulator compensates for any changes in the characteristics of the drive caused by changes in load or by outside influences such as line voltage and ambient temperature. With a closed loop speed regulator, the most important characteristic of the drive is its ability to rapidly respond to changes in requirements for torque.

There are many types of controllers; each of them has a specified function to do. The P, PI, PD and PID are the basic types of controllers. Also the PID controller can be divided into parallel PID and series PID controller. The success of the PID controllers is also enhanced by the fact that they often represent the fundamental component for more sophisticated control schemes that can be implemented when the basic control law is not sufficient to obtain the required performance or a more complicated control task is of concern. [11]

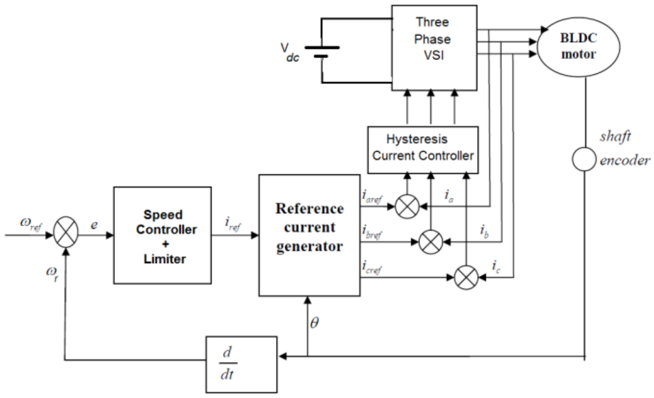

Fig.5 Speed Controller

2.5.1 P, PI, PID Speed controllers:

Proportional controller amplifies the error by multiplying it by some proportional constant. The error generated is small, but not zero. Therefore, P Controller generates a permanent error or offset or steady state error each time the controller responds to load.

A PI controller can cause closed loop instability if integral action is too aggressive. The controller may over correct for an error and create a new one of even greater magnitude in the opposite direction.

Compared to two term PI controller, a PID controller can even appear to anticipate the level of effort that is ultimately required to maintain the process variable at a new set point. Derivative action adds a dramatic spike or kick to the controllers output in the case of an abrupt change in the error due to new set point.

2.5.2 Different PID Tuning methods:

Many various tuning methods have been proposed from 1942 up to now for gaining better and more acceptable control system response based on our desirable control objectives such as percent of overshoot, integral of absolute value of the error (IAE), settling time, manipulated variable behavior and etc. Some of these tuning methods have considered only one of these objectives as a criterion for their tuning algorithm and some of them have developed their algorithm by considering more than one of the mentioned criterion. [11] The PID controller tuning methods are classified into two main categories.

- Closed loop methods
- Open loop methods

Closed loop tuning techniques refer to methods that tune the controller during automatic state in which the plant is operating in closed loop. The open loop techniques refer to methods that tune the controller when it is in manual state and the plant operates in open loop. Some of the tuning methods considered for the simulation are listed as below:

Closed loop methods are:

-Ziegler-Nichols method

-Tyreus-Luyben method

Open loop methods are:

-Open loop Ziegler-Nichols method

-C-H-R method

-Cohen and Coon method

Let the transfer function of the PID controller be

$$G_c(s) = k_c\left(1 + \frac{\tau_i}{s} + \tau_d s\right) \quad (25)$$

where, k_c- Proportional gain

τ_i- Integral time

τ_d- Derivative time

2.5.2.1 Closed loop Ziegler-Nichols Method:

This method is a trial and error tuning method based on sustained oscillations that was first proposed by Ziegler and Nichols (1942). This method that is probably the most known and the most widely used method for tuning of PID controllers is also known as online or continuous cycling or ultimate gain tuning method.

Steps to apply closed loop Z-N tuning:

1. Connect the controller to the plant, turn off the integral control, i.e. set τ_i=0, and turn off the derivative control by setting τ_d=0.
2. Start raising the gain k_c until the process starts to oscillate as shown in fig.6. The gain where this occurs is k_u and the period of the oscillations is τ_u.
3. Record the values as ultimate gain (k_u) and period (τ_u).
4. Evaluate control parameters as prescribed by Ziegler and Nichols.

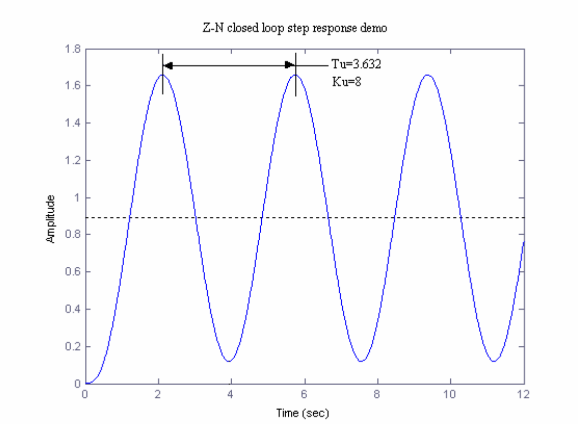

Fig.6 Z-N closed loop parameter evaluation for sample system

TABLE II. CONTROLLER PARAMETERS FOR CLOSED LOOP Z-N METHOD

Controller type	Parameters		
	k_p	τ_i	τ_d
P	0.5	-	-
PI	0.45	/1.2	-
PID	0.6	/2	/8

2.5.2.2 Tyreus-Luyben method:

The Tyreus-Luyben procedure is quite similar to the Ziegler–Nichols method but the final controller settings are different. Also this method only proposes settings for PI and PID controllers. These settings that are based on ultimate gain and period are given in Table 3. Like Z-N method this method is time consuming and forces the system to margin if instability.

TABLE III. CONTROLLER PARAMETERS FOR T-L METHOD

Controller type	Parameters		
	k_p	τ_i	τ_d
PI	/3.2	2.2	-
PID	/3.2	2.2	/6.3

2.5.2.3 Open loop Zeigler-Nichols Method:

This method was based on the plant reaction to a step input and characterized by two parameters. The method is often referred to as the Open Loop, or Step Response tuning method. The parameters, a and L, are determined by applying a unit step function to the process.

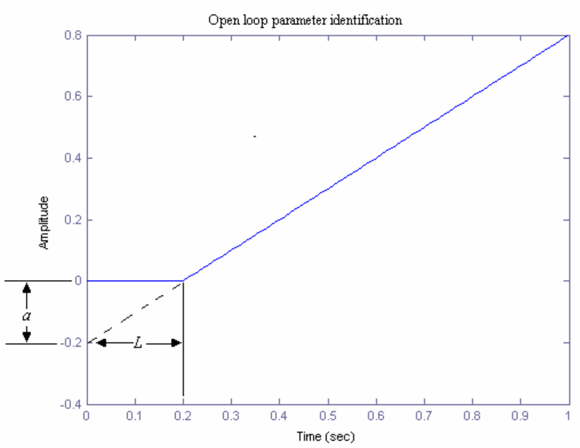

Fig.7 Open loop parameter identification

Referring to Fig.7, the point where the slope of the step response has its maximum is first determined. Then the tangent at this point is drawn. The intersection of this tangent and vertical axis at T=0 gives the parameters a and L. Ziegler and Nichols derived PID parameters directly as functions of a and L. The results are given in Table 4.

TABLE IV. CONTROLLER PARAMETERS FOR OPEN LOOP Z-N METHOD

Controller type	Parameters		
	k_p	τ_i	τ_d
P	1/a	-	-
PI	0.9/a	3L	-

Controller type	Parameters		
	k_p	τ_i	τ_d
PID	1.2/a	2L	L/2

2.5.2.4 Chien, Hrones and Reswick (C-H-R) Tuning Method:

This method of tuning was derived from the original Ziegler-Nichols Open Loop method with the intention of obtaining the quickest response without overshoot and quickest response with 20% overshoot. To tune the controller according to the C-H-R method, the parameters *a*, *L*, and *T* (the time constant of the of the plant transfer function, which is the time it takes for the system to reach 63% of its final value) are determined. The C-H-R method yields Table 5 for 0% overshoot.

TABLE V. CONTROLLER PARAMETERS FOR C-H-R TUNING METHOD WITH 0% PEAK OVERSHOOT

Controller type	Parameters		
	k_p	τ_i	τ_d
P	0.3/a	-	-
PI	0.35/a	1.2T	-
PID	0.6/a	T	0.5/L

2.5.2.5 Cohen-Coon Method:

This tuning method has been discovered almost after a decade than the Ziegler-Nichols method. Cohen-Coon tuning requires three parameters a, L and T which are obtained in the same procedure as open loop Z-N method. The controller parameters are derived directly as functions of a, L and T. The results are given in Table 6 below.

TABLE VI. CONTROLLER PARAMETERS FOR C-C TUNING METHOD

Controller type	Parameters		
	k_p	τ_i	τ_d
P	$\frac{T}{a}(1+\frac{L}{3T})$	-	-
PI	$\frac{T}{a}(\frac{0.9+L}{12T})$	$\frac{L(30+\frac{3L}{T})}{9+\frac{20L}{T}}$	-
PID	$\frac{T}{a}(\frac{16T+30}{12T})$	$\frac{L(32+\frac{6L}{T})}{13+\frac{8L}{T}}$	$\frac{4L}{11+\frac{2L}{T}}$

2.5.3 Adaptive Control Techniques:

Adaptive control use to change the control algorithm coefficients in real time to compensate for variations in environment or in the system itself. In drives, electrical and mechanical parameters do not remain constant. A sudden increase of T_l or J reduces speed. These effects can be reduced by high gain negative feedback loop. But this may cause under damping or instability[5]. Therefore real time adaptation of the controller is required.

Different adaptive control techniques are:

1) Self tuning control
2) MRAC
3) Sliding mode control
4) Expert system control
5) Fuzzy control
6) Neural network control

One of the most successful expert system techniques applied to a wide range of control applications has been the Fuzzy Set Theory, which has made possible the establishment of "intelligent control".

2.6 Adaptive Fuzzy Controller

Conventional PID controllers are generally insufficient to control process with additional complexities such as time delays, significant oscillatory behavior (complex poles with small damping), parameter variations, non-linearities and MIMO plants. Fuzzy logic has rapidly become one of the most successful of today's technology for developing sophisticated control system. The past few years have witnessed a rapid growth in number and variety of applications of fuzzy logic. Many decision-making and problem solving tasks are too complex to understand quantitatively, however, people succeed by using knowledge that is imprecise rather than precise. Fuzzy logic is all about the relative importance of precision. Fuzzy logic has two different meanings: in a narrow sense, fuzzy logic is a logical system which is an extension of multi valued logic, but in wider sense, fuzzy logic is synonymous with the theory of fuzzy[3].

In industrial electronics the FLC control has become an attractive solution in controlling the electrical motor drives with large parameter variations like machine tools and robots. However, the FLC design and tuning process is often complex because several quantities, such as membership functions, control rules, input and output gains, etc must be adjusted[11]. The design process of a FLC can be simplified if some of the mentioned quantities are obtained from the parameters of a given Proportional-Integral controller for the same application.

Fuzzy logic controllers are designed particularly for non-linear dynamic systems with many inputs and outputs which are so complex, that it is very difficult or even impossible to build exact mathematical model. Fuzzy logic expressed operational laws in linguistics terms instead of mathematical equations.

The basic structure of a fuzzy logic controller is shown in Fig.8. Its fundamental components are Fuzzification, control rule base, inference mechanism and defuzzification.

2.6.1 Fuzzification:

The following functions are performed in the Fuzzification process:

1. Multiple measured crisp inputs first must be mapped into fuzzy membership function this process is called fuzzification.
2. Performs a scale mapping that transfers the range of values of input variables into corresponding universes of discourse.
3. Performs the function of fuzzification that converts input data into suitable linguistic values which may be viewed as labels of fuzzy sets.

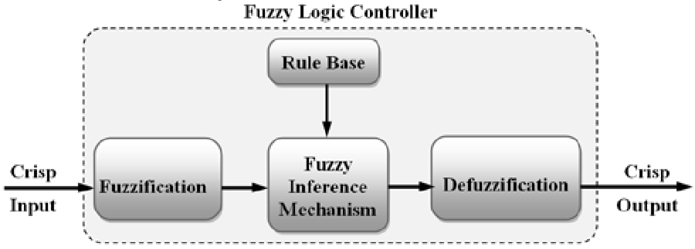

Fig.8 The structure of a fuzzy logic controller

Fuzzy logic linguistic terms are often expressed in the form of logical implication, such as if then rules[3]. These rules define a range of values known as fuzzy member ship functions. Fuzzy membership function may be in the form of a triangular, trapezoidal, bell (as shown in Fig.9) or another appropriate from.

The triangle membership function is defined by the limits V_{al1}, V_{al2} and V_{al3} as,

$$\mu(u_i) = \begin{cases} \dfrac{u_i - V_{al1}}{V_{al2} - V_{al1}}, & V_{al1} \le u_i \le V_{al2} \\ \dfrac{V_{al3} - u_i}{V_{al3} - V_{al2}}, & V_{al2} \le u_i \le V_{al3} \\ 0, & otherwise \end{cases}$$

Trapezoidal membership function is defined by the limits V_{al1}, V_{al2}, V_{al3} and V_{al4} as,

$$\mu(u_i) = \begin{cases} \dfrac{u_i - V_{al1}}{V_{al2} - V_{al1}}, & V_{al1} \le u_i \le V_{al2} \\ 1, & V_{al2} \le u_i \le V_{al3} \\ \dfrac{V_{al4} - u_i}{V_{al4} - V_{al3}}, & V_{al3} \le u_i \le V_{al4} \\ 0, & otherwise \end{cases}$$

The bell membership functions are defined by parameters X_p, w and m as follows

$$\mu(u_i) = \frac{1}{\left[1 + \left(\frac{|u_i - X_p|}{w}\right)^{2m}\right]}$$

where, X_p is the midpoint and w is the width of bell function, m≥1, and describe the convexity of the bell function.

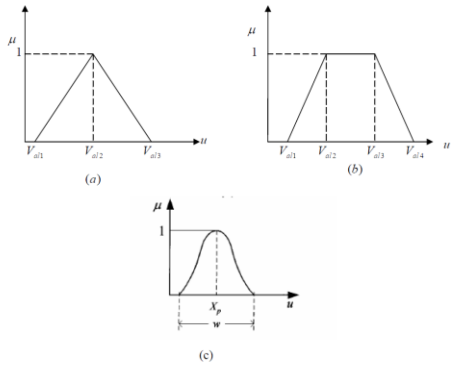

Fig.9 (a) Triangular (b) Trapezoidal (c) Bell shape membership functions

The inputs of the fuzzy controller are expressed in several linguistic levels. These levels can be described as Positive Big (PB), Positive Medium (PM), Positive Small (PS), Zero (Z), Negative Small (NS), Negative Medium (NM), Negative Big (NB) or in other levels. Each level is described by fuzzy set.

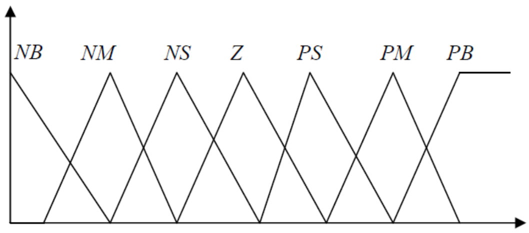

Fig. 10 Seven levels of Fuzzy membership functions

2.6.2 Fuzzy Inference:

Fuzzy inference is the process of formulating the mapping from a given input to an output using fuzzy logic. The mapping then provides a basis from which decisions can be made, or patterns discerned[11]. There are two types of fuzzy inference systems that can be implemented in the Fuzzy Logic Toolbox: Mamdani-type and Sugeno-type. These two types of inference systems vary somewhat in the way outputs are determined.

Fuzzy inference systems have been successfully applied in fields such as automatic control, data classification, decision analysis, expert systems, and computer vision. Because of its multidisciplinary nature, fuzzy inference systems are associated with a number of names, such as fuzzy-rule-based systems, fuzzy expert systems, fuzzy modeling, fuzzy associative memory, fuzzy logic controllers, and simply (and ambiguously) fuzzy. Mamdani's fuzzy inference method is the most commonly seen fuzzy methodology. Mamdani's method was among the first control systems built using fuzzy set theory[10]. The second phase of the fuzzy logic controller is its fuzzy inference where the knowledge base and decision making logic reside. The rule base and data base from the knowledge base. The data base contains the description of the input and output variables. The decision making logic evaluates the control rules, the control rule base can be developed to relate the output action of the controller to the obtained inputs.

2.6.3 Defuzzification:

The output of the inference mechanism is fuzzy output variables. The fuzzy logic controller must convert its internal fuzzy output variables into crisp values so that the actual system can use these variables. This conversion is called defuzzification. The commonly used control defuzzification strategies are

(a) The MAX criterion method:
The max criterion produces the point at which the membership function of fuzzy control action reaches a maximum value.

(b) The height method:
The centroid of each membership function of each rule is first evaluated. The final output U_0 is then calculated as the average of the individual centroids, weighted by their heights as follows:

$$U_0 = \frac{\sum_{i=1}^{n} u_i \mu(u_i)}{\sum_{i=1}^{n} \mu(u_i)}$$

(c) The centroid method (or) Centre of Area method (COA):
The widely used centroid strategy generates the centre of gravity of area bounded by the membership function curve.

$$\bar{y} = \frac{\int \mu_Y(y).ydy}{\int \mu_Y(y)dy}$$

2.6.4 Fuzzy Rule base:

The set of linguistic rules is the essential part of a fuzzy controller. In many cases it's easy to translate an expert's experience into these rules and any number of such rules can be created to define the actions of the controller. In the designed fuzzy system, conventional fuzzy conditions and relations such as "If e is A and Δe is B, then Δk is C" are used to create the fuzzy rule base (7 x 7).

TABLE VII. FUZZY RULE BASE FOR ΔK

e/Δe	NB	NM	NS	Z	PS	PM	PB
NB	NB	NB	NB	NB	NM	NS	Z
NM	NB	NB	NB	NM	NS	Z	PS
NS	NB	NB	NM	NS	Z	PS	PM
Z	NB	NM	NS	Z	PS	PM	PB
PS	NM	NS	Z	PS	PM	PB	PB
PM	NS	Z	PS	PM	PB	PB	PB
PB	Z	PS	PM	PB	PB	PB	PB

III. TRANSFER FUNCTION MODEL

3.1 BLDC motor and Load

The motor contains an inner loop due to induced emf. The inner current loop will cross this back emf loop, creating a complexity in the development of the model. The interactions of these loops can be decoupled by suitably redrawing the block diagram. The load is assumed to be proportional to speed as in [4].

$$T_l = B_l \omega_m$$

The voltage equation per phase is

$$V_a = R_a i_a + (L - M)\frac{di_a}{dt} + e_a$$

Taking Laplace Transform of the above equation and neglecting the initial conditions,

$$i_a = \frac{V_a - e_a}{s(L - M) + R_a}$$

Electromagnetic torque equation is

$$T_e = T_l + J\frac{d\omega_m}{dt} + B\omega_m$$

$$\omega_m = \frac{T_e - T_l}{sJ + B}$$

$$T_e = \frac{e_a i_a}{\omega_m} \qquad \text{where, } e_a = k_b \omega_m$$

The overall transfer function of motor and load can be derived as follows:

$$\frac{\omega_m(s)}{V_a(s)} = \frac{\omega_m(s)}{I_a(s)} \frac{I_a(s)}{V_a(s)}$$

If $B + B_l \cong B, \ then \ \frac{\omega_m(s)}{T_e(s)} = \frac{1}{sJ + B}$

$$\therefore \frac{\omega_m(s)}{I_a(s)} = \frac{K_t}{sJ + B}$$

$$Let \ \tau_m = \frac{J}{B} \ then, \quad \frac{\omega_m(s)}{I_a(s)} = \frac{K_t/B}{s\tau_m + 1}$$

$$\frac{I_a(s)}{V_a(s)} = \frac{\frac{1}{s(L - M) + R_a}}{1 + \frac{k_b k_t}{s(L - M) + R_a} \frac{1}{B(1 + s\tau_m)}}$$

$$Let \ L - M = L_a, \ K_1 = B, \ \frac{-1}{\tau_1}, \frac{-1}{\tau_2} = \frac{-1}{2}\left(\frac{R_a}{L_a} + \frac{B}{J}\right) \pm \sqrt{\frac{1}{4}\left(\frac{R_a}{L_a} + \frac{B}{J}\right)^2 - \left(\frac{K_b K_t + R_a B}{J L_a}\right)}$$

$$\frac{I_a(s)}{V_a(s)} = \frac{(1 + s\tau_m)K_1}{(1 + s\tau_1)(1 + s\tau_2)}$$

3.2 Inverter

Inverter is modeled as a gain with time lag. The transfer function model of an inverter is

$$G_r(s) = \frac{K_{in}}{1 + sT_{in}}$$

$$K_{in} = \frac{\left(\frac{2V_{dc}}{\pi}\right)}{V_{cm}} = \frac{0.65V_{dc}}{V_{cm}}$$

where,

$$T_{in} = \frac{1}{2f_c}$$

V_{dc}- DC link voltage input to inverter
V_{cm}- Maximum control voltage
f_c– Switching or carrier frequency

3.3 Current loop

H_c is the current feedback gain
Using Block diagram reduction rules, the t

function $\frac{I_a(s)}{I_a^*(s)}$ is obtained as follows:

$$\frac{I_a(s)}{I_a^*(s)} = \frac{K_1K_{in}(1+sT_m)}{(1+sT_{in})(1+sT_1)(1+sT_2)+K_{in}K_1}$$

In order to approximate the transfer functio second order for simple control, the follo approximations are made near the vicinity o crossover frequency:

$$1 + sT_m \cong sT_m$$

Also,

$$(1+sT_1)(1+sT_2) \cong (1+sT_a), where\ T_a$$

$$\frac{I_a(s)}{I_a^*(s)} = \frac{K_1K_{in}sT_m}{(1+sT_{in})(1+sT_a)+K_{in}K_1H_csT_m}$$

Let, $T_a + T_{in} \cong T_{av}$

$$\frac{I_a(s)}{I_a^*(s)} = \frac{(K_1K_{in}T_m)s}{s^2(T_aT_{in})+s(T_{av}+K_{in}K_1H_cT_m)+1}$$

$$\frac{I_a(s)}{I_a^*(s)} = \frac{(K_1K_{in}T_m)s}{(1+sT_p)(1+sT_q)}$$

Where,

$$\frac{-1}{T_p}, \frac{-1}{T_q} = -\left[\frac{T_{av}+K_{in}K_1H_cT_m}{2T_aT_{in}}\right] + \sqrt{\frac{(T_{av}+K_{in}K_1H_cT_m)^2}{4(T_aT_{in})^2} - \frac{1}{}}$$

On further approximations,

$$\frac{I_a(s)}{I_a^*(s)} = \frac{(K_1K_{in}T_m)}{(1+sT_p)T_q}$$

$$\therefore The\ approximate\ current\ loop\ transfer\ function\ is\ \frac{I_a(s)}{I_a^*(s)} = \frac{1}{(1+sT_i)}$$

$$where, K_i = \frac{K_1K_{in}T_m}{T_q};\ T_i = T_p$$

The overall speed control loop is then derived from the above transfer functions using a PID speed controller and limiter.

IV. MATLAB/SIMULINK MODELS

For a BLDC motor with the following specifications, the overall closed loop transfer function of the drive is obtained as follows:
0.5HP, 160V, 700rpm, 3-Φ BLDC motor with P=4; R_a=0.7Ω/ph; L=0.0272H; M=0.015H; K_b=0.5128V/ rad/ sec; K_t=0.49N-m/A; J=0.0002kg-m/s^2; B=0.02N-m/ rad /sec; f_c=2KHz; V_{cm}=10V

4.1 Mathematical model of the BLDC Drive

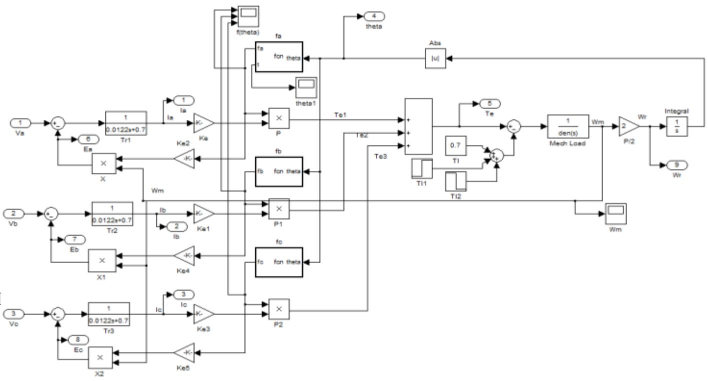

Fig. 12 Simulink model of BLDC Motor

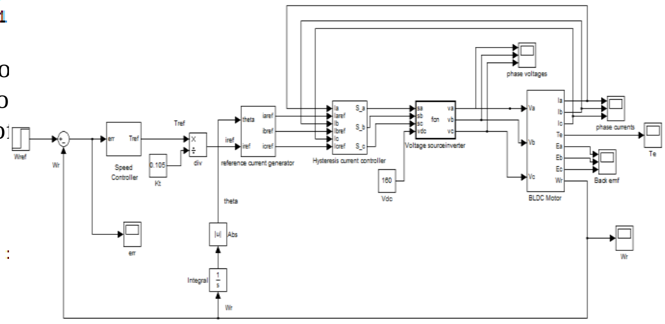

Fig. 13 Overall Closed loop model of the drive

4.2 Transfer function model

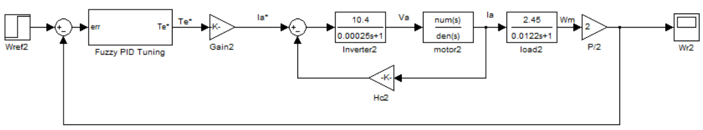

Fig. 14 Closed loop Transfer function of the BLDC Motor Drive

4.3 Speed Controller

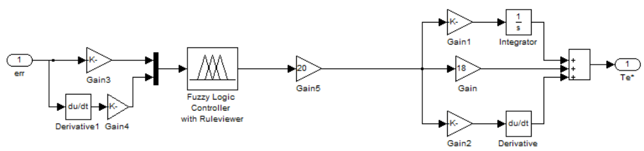

Fig. 15 Fuzzy PI Controller

V. RESULTS

Conventional PI controller tuning methods are applied to the transfer function model of the drive first and the results it is observed that closed loop control techniques give better response for a step change in input compared to open loop techniques. To reduce the peak overshoots, the results were then compared with adaptive fuzzy control technique. The fuzzy PID controller is further tuned with the above closed loop control techniques and it is observed that closed loop Tyreus-Lyuben tuning method with fuzzy controller gives better response with zero peak overshoot and zero steady state error. The comparision of responses between different control techniques were listed in the table 8 below.

TABLE VIII. COMPARISION OF DIFFERENT TUNING METHODS FOR TRANSFER FUNCTION MODEL OF THE DRIVE

Controller type	Responses			
	Rise time (sec)	*Settling time (sec)*	*Peak oevrshoot (rad/sec)*	*Steady state error (rad/sec)*
Without Controller	0.002	0.004	12.462	5.795
PID Controller	0.0068	0.0212	6.667	0
Z-N Open loop PI Controller	0.00214	0.0338	40.567	0
Cohen –Coon tuned PID Controller	0.000964	0.0283	46.667	0
C-H-R tuned PI Controller	0.063	0.115	0	0
Z-N Closed loop PI Controller	0.000569	0.0102	43.937	0
Tyreus-Luyben PI Controller	0.000745	0.0061	24.887	0
Adaptive Fuzzy PID Controller	0.0068	0.0212	0	3.2×10^{-3}
Adaptive Fuzzy+Z-N Closed loop PI Controller	0.00161	0.0122	0	0
Adaptive Fuzzy+T-L PI Controller	0.00161	0.0122	0	0

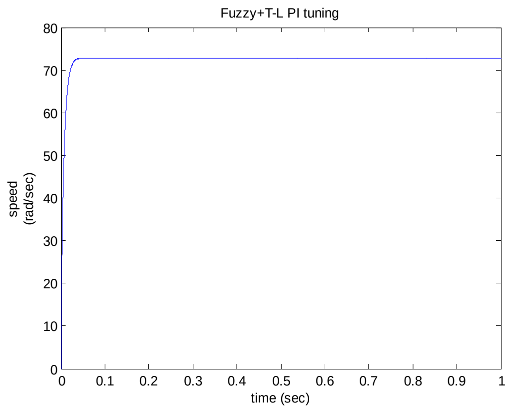

Fig. 16 The speed response with Fuzzy PI Controller

The above control techniques were then applied on the mathematical model of the drive and it is observed that Adaptive fuzzy PI control technique with Tyreus-Lyuben tuning serves as a better controller with zero steady state error and reduced settling time. The comparison of the different controllers is tabulated below in table 9 and the responses were plotted.

TABLE IX. COMPARISION OF DIFFERENT TUNING METHODS FOR MATHEMATICAL MODEL OF THE DRIVE

Controller type	Responses			
	Rise time (sec)	*Settling time (sec)*	*Peak overshoot (rad/sec)*	*Steady state error (rad/sec)*
Z-N Closed loop PI Controller	0.0025	0.004	0.05	0.383
Tyreus-Luyben PI Controller	0.003	0.004	0.124	0.507
Adaptive Fuzzy Controller	0.02	0.03	0	2.633
Adaptive Fuzzy+Z-N Closed loop PI Controller	0.015	0.03	0	1.518
Adaptive Fuzzy+T-L PI Controller	0.02	0.03	0	0.1085

From the results, it is clear that Adaptive Fuzzy + Tyreus-Luyben tuned PI Controller gives better response with zero peak overshoot and very less steady state error. Also, the torque response of the drive with this control is a smooth curve compared to the remaining controllers.

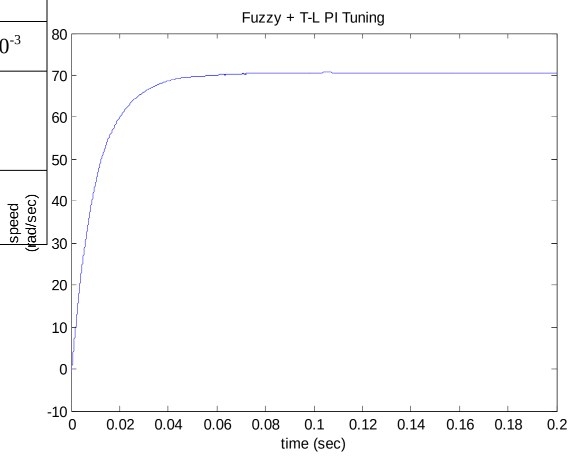

Fig. 17 Speed response of the Drive

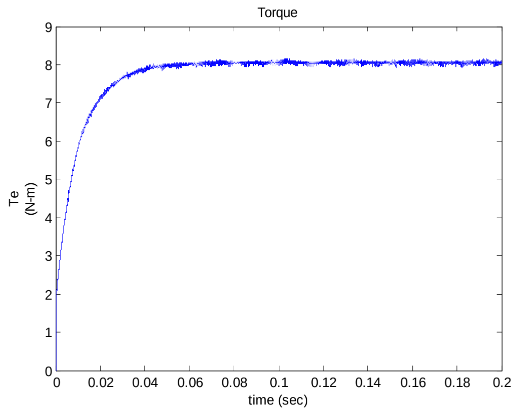

Fig.18 Electromagnetic torque developed in the drive

If there is a sudden change in the load, the controller must be able to withstand the load change without any change in speed. A sudden change in load is applied to the simulation at 0.2sec and at 0.3sec and the results are as shown below:

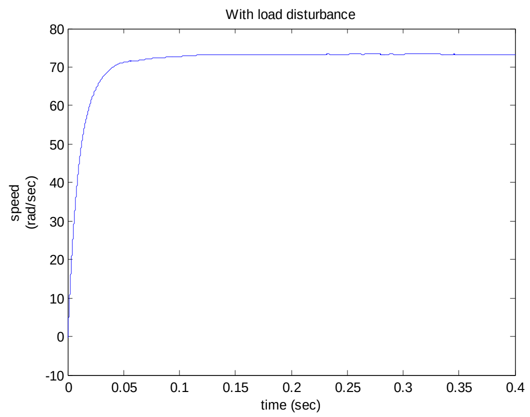

Fig. 19 Speed resposne of the drive with load disturbance

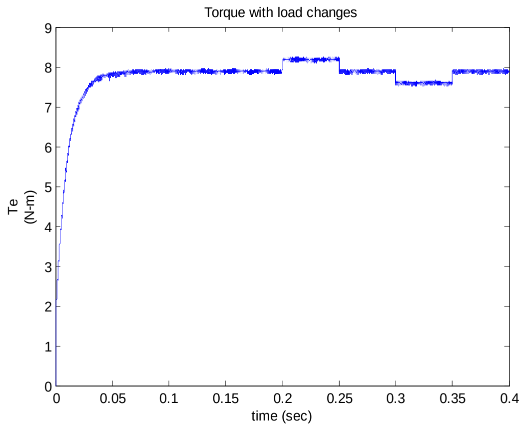

Fig.20 Torque developed in the drive with load disturbance

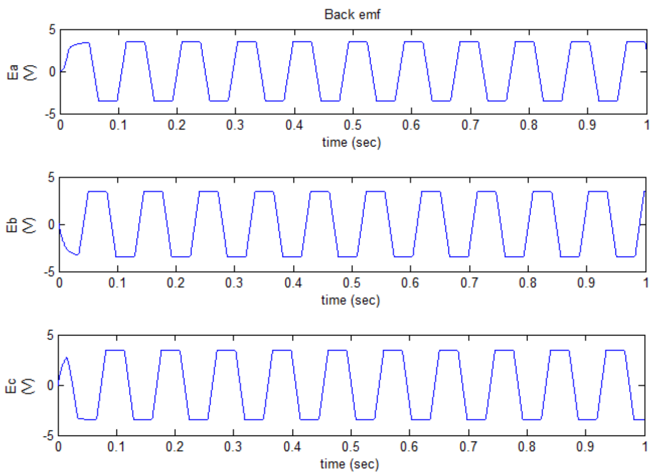

Fig.21 3-ΦTrapezoidal Back emf Waveform of the BLDC motor

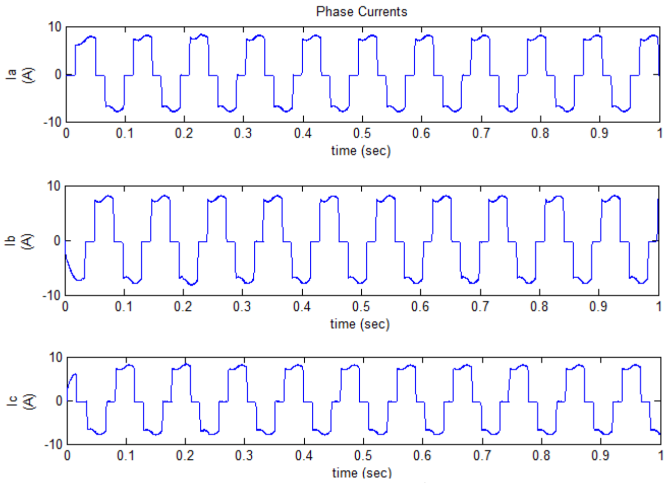

Fig.22 Three phase currents of the BLDC motor

VI. CONCLUSION

Conventional P/PI/PID controllers and fuzzy tuned P/PI/PID controllers are the Six control techniques which are used to control the Speed of BLDC drive. Rule base for the fuzzy tuned P/PI/PID techniques are designed for two inputs i.e error and change in error and one output i.e change in the gain. For inputs, 7 membership functions and for output also seven membership functions and totally 49 rules are designed. Different PID Tuning methods have been applied on the transfer function model of the BLDC drive and the results were compared with the actual mathematical model of the drive. It is observed that the delay time is reduced, rise time is increased and settling time is reduced to more than half for fuzzy tuned PI controller when compared to conventional PI controller. Transient and steady state responses are improved by using fuzzy tuned controllers than using the conventional controllers.

VII. FUTURE SCOPE

There are a large number of possible avenues for advancement of control of BLDC drives. A major research area is that of sensor less control. This typically means that measures have been taken to eliminate the expensive rotor position sensor, but not necessarily current or voltage sensors.

In short, the BLDC motor drive is an effective in high-performance drive applications. Rapid torque response is readily achieved as vector control of BLDC drives is much more straight forward than it is for induction motor drives. The capital cost can be high, but the high efficiency can at least partially offset this in high-power applications. For these reasons, the BLDC drive is expected to continue to be competitive for the near future.

For attaining better results, Work can be extended by adding Neuro-Fuzzy technique to the system. The two tools are successfully combined to maximize their individual strengths. The field of Neuro-Fuzzy technology plays a key role in controlling Motor drives. The present work is concluded with sophisticated applications of BLDC drive control.

REFERENCES

[1.] Padmaraja Yedamale, "Brushless DC (BLDC) Motor Fundamentals", Microchip Technology Inc.
[2.] Mehmet Cunkas and Omer Aydogdu, "Realization of fuzzy logic controlled brushless dc motor drives using Matlab / Simulink", Mathematical and Computational Applications, Vol. 15, No. 2, pp. 218-229, 2010. Association for Scientific Research.
[3.] S.Rambabu and Dr. B. D. Subudhi, "Modeling And Control Of A Brushless DC Motor", National Institute of Technology, Rourkela.
[4.] R. Krishnan, "Electric motor drives, modeling analysis and control", Prentice Hall publications.
[5.] B.K. Bose, "Modern Power Electronics and A.C Drives", Prentice Hall PTR publications.
[6.] Dennis Fewson, "Introduction to Power Electronics", Essential Electronics Series.
[7.] Module 5, DC to AC Converters Version 2 EE IIT, Kharagpur
[8.] BLDC Motor Modelling and Control – A Matlab/Simulink Implementation" by Stefan Baldursson, International masters program in Electric Power Engineering, Chalmers University.
[9.] Madhusudan Singh and Archna Garg, "Performance Evaluation of BLDC Motor with Conventional PI and Fuzzy Speed Controller", Electrical Engineering Department, Delhi Technological University.
[10.] Chuen Chien Lee, "Fuzzy Logic in Control Systems-Fuzzy Logic Controllers", Student Member, IEEE, IEEE Transcations on systems, Man, and Cybernetics, Vol.20, No.2, March/April 1990.
[11.] Pooja Agarwal and Arpita Bose, "Brushless Dc Motor Speed Control Using Proportional-Integral And Fuzzy Controller", IOSR Journal of Electrical and Electronics Engineering (IOSR-JEEE) e-ISSN: 2278-1676,p-ISSN: 2320-3331, Volume 5, Issue 5 (May. - Jun. 2013), PP 68-78
[12.] Jan Jantzen, "Tuning Of Fuzzy PID Controllers", Technical University of Denmark, Department of Automation, Bldg 326, DK-2800 Lyngby, DENMARK. Tech. report no 98-H 871 (fpid), April 16, 1999.
[13.] "High Performance Drives -- speed and torque regulation" Technical Guide No.100, ABB Industrial Systems Inc., New Berlin, USA